JOURNAL OF CATALYSIS 138, 547–561 (1992)

Investigation of the Surface Structure and Basic Properties of Calcined Hydrotalcites

ANDREW L. MCKENZIE,[1] CHRISTOPHER T. FISHEL, AND ROBERT J. DAVIS[2]

Department of Chemical Engineering, University of Virginia, Charlottesville, Virginia 22903-2442

Received April 9, 1992; revised June 22, 1992

In this work, we investigated the influence of preparation method, calcination temperature, and Mg : Al atomic ratio on the basic properties of calcined hydrotalcites. The steady-state decomposition of 2-propanol at 593 K and atmospheric total pressure was studied to compare the surface reactivities of the mixed oxides with those of pure MgO and Al_2O_3. In general, the activity and selectivity to propanone formation followed the order MgO ≥ calcined hydrotalcities ≫ alumina, indicating that catalytically active basic sites are present on the calcined hydrotalcites. However, the selectivity to propanone is influenced significantly by the method of hydrotalcite synthesis. In addition, the observed activation energies and pre-exponential factors for propanone formation compensated each other over mixed oxides of different Mg : Al atomic ratios, resulting in similar areal reaction rates. The observed compensation effect can be explained by a shift in the rate-determining elementary step on a nonuniform surface. No significant influence of calcination temperature on the surface area and 2-propanol reactivity of hydrotalcite was observed for temperatures of 723–923 K, whereas calcination of hydrotalcite at 1173 K resulted in lower surface area, decreased selectivity to propanone, and formation of separate oxide phases. Temperature-programmed desorption (TPD) of CO_2 from calcined hydrotalcites indicated that the incorporation of aluminum into MgO suppresses the formation of high-strength base sites normally associated with pure MgO; however, low-strength base sites are still present on the mixed oxide. Based on results from ^{27}Al NMR, XPS, CO_2 TPD, and 2-propanol reaction, we speculate that some Al is located at the surface but is in a local oxidic environment not favorable for acid-catalyzed reactions that typically occur over pure alumina.

INTRODUCTION

Hydrotalcite, or magnesium–aluminum hydroxycarbonate, is a naturally occurring anionic clay that reversibly decomposes upon calcination at high temperature to form a high-surface-area, basic, mixed oxide. The structure of hydrotalcite is similar to that of brucite, $Mg(OH)_2$, where Mg^{2+} is octahedrally coordinated to the surrounding hydroxide ions. These magnesium hydroxide octahedra share adjacent edges to form sheets or layers. In hydrotalcite, some of the magnesium is isomorphously replaced by Al^{3+} and the atomic ratio of magnesium to aluminum can be quite variable. However, values between 1.7 and 4.0 are usually reported for Mg : Al atomic ratios in synthetic samples. Recently, Shaper *et al.* synthesized relatively pure hydrotalcite with an Mg : Al ratio of 10 by strictly controlling coprecipitation conditions (*1*). Substitution of Al^{3+} for Mg^{2+} produces net positive charges on the metal hydroxide layers because the Al^{3+} remains octahedrally coordinated to the hydroxyl groups. This layer charge in naturally occurring hydrotalcite is balanced by interlayer carbonate. Therefore, hydrotalcites are capable of simple anion-exchange reactions and one area of current research with hydrotalcites is pillaring the layers with large anions to increase the interlayer spacing (*2, 3*). In addition to anions, water molecules are also located between the metal hydroxide layers.

The changes that occur during thermal

[1] Current address: Exxon Research and Engineering, Florham Park, NJ 07932.

[2] To whom correspondence should be addressed.

0021-9517/92 $5.00

decomposition of hydrotalcite have been described previously by Reichle *et al.* (*4*) and Miyata (*5*). With increasing temperature, interlayer water is lost first, followed by dehydroxylation and decomposition of interlayer carbonate to CO_2. Removal of CO_2 and structural water from calcined hydrotalcite is accompanied by a modest increase in specific surface area, ultimately yielding mixed oxides of 200–300 $m^2\ g^{-1}$. In addition, the X-ray diffraction pattern of the resulting oxide indicates a diffuse MgO structure with no separate crystalline phases.

Calcined hydrotalcites are potentially useful as base catalysts and catalyst supports since the high surface area is stable to steam treatment (*1*). These materials are active for typically base-catalyzed reactions including aldol condensation of propanone (*6*), double bond migration (*1, 6*), H–D exchange of propanone and toluene (*6*), β-propiolactone polymerization (*7*), 2-propanol decomposition (*8*), and condensation of benzaldehyde (*9*). Calcined hydrotalcite has also been used as a novel support for Pt clusters in the catalytic aromatization of *n*-hexane (*10, 11*). Hydrotalcite synthesis, characterization, and catalytic function have been recently reviewed by Cavani *et al.* (*12*).

This work describes the synthesis, characterization, and reaction of 2-propanol over a series of thermally treated hydrotalcites, magnesia and alumina. Characterization techniques include X-ray diffraction, elemental analysis, N_2 adsorption, temperature-programmed desorption of CO_2, ^{27}Al NMR spectroscopy, and X-ray photoelectron spectroscopy. The decomposition of 2-propanol was used to probe relative surface acidity and basicity of the materials, since 2-propanol usually dehydrogenates to form propanone over basic catalysts and dehydrates to form propene over acidic catalysts (*13, 14*).

EXPERIMENTAL METHODS

Preparation of Hydrotalcite and Hydroxide Samples

Hydrotalcite samples were prepared by coprecipitating an aqueous solution of magnesium and aluminum salts with a highly basic carbonate solution (*10, 11*). The former solution contained $Mg(NO_3)_2 \cdot 6H_2O$ and $Al(NO_3)_3 \cdot 9H_2O$ dissolved in distilled, deionized water at Mg : Al molar ratios of 5 : 1, 3 : 1, and 2 : 1. The second solution contained appropriate amounts of KOH and $K_2CO_3 \cdot 1.5H_2O$ so that the Al : CO_3^{2-} molar ratio was equal to 2 and the pH of the final solution was 8–10. Another series of hydrotalcites was prepared with basic solutions of NaOH and Na_2CO_3 instead of the corresponding potassium compounds; however, most of the results presented are for the samples prepared with K. All of the compounds listed above were from Aldrich (ACS Reagent Grade), except NaOH which was from Fisher (Certified ACS Grade). The precipitation was carried out by dropwise addition of the two solutions at 333 K followed by stirring overnight at 333 K. The resulting white precipitate was both filtered and washed with boiling, distilled, deionized water three times and was then dried in air at 373 K. Hereafter, the hydrotalcites and the materials used in preparation are identified by the approximate magnesium to aluminum ratios, e.g., HT5 : 1–K or HT5 : 1–Na. Magnesium hydroxide and aluminum hydroxide were also precipitated separately by the addition of aqueous potassium hydroxide to a magnesium nitrate solution and an aluminum nitrate solution, respectively. In addition, an MgO sample from Ube Industries was also studied (*15*).

Characterization of Catalysts

Bulk elemental analyses of the hydrotalcites for magnesium and aluminum were performed by Galbraith Laboratories. Additionally, some of these samples were analyzed for Na or K, which are possible impurity cations from the synthesis procedure. The surface compositions of some of the calcined materials were also estimated from X-ray photoelectron spectroscopy. The samples were also examined with a Scintag X-ray diffractometer using Cu$K\alpha_1$ radiation at a scan rate of 1–2 degrees per minute.

Specific surface areas were determined from N_2 adsorption by applying the BET formalism. Magic-angle-spinning ^{27}Al NMR spectra were recorded with a Bruker MSL 300 spectrometer operating at 78.171 MHz with sample spinning rates of 9–12 kHz. The chemical shifts are reported relative to a 1 *M* aqueous solution of $Al(NO_3)_3$ and are not corrected for second-order quadrupolar effects.

Temperature-programmed desorption (TPD) of preadsorbed CO_2 from the catalysts was used to estimate the density of surface base sites. An atmospheric pressure flow system with a quadrupole mass spectrometer was used for the experiment. First, a fresh catalyst sample was heated at a rate of 4 K min^{-1} in flowing He and then calcined in He for 4 h at 823 K. The release of CO_2 from hydrotalcite during decomposition was monitored by the mass spectrometer. Following calcination, the sample was cooled to room temperature (RT) and exposed to flowing CO_2 (Air Products, 99.99%) for 0.5 h. The system was then purged with He carrier gas to remove weakly adsorbed CO_2. The temperature of the sample was increased linearly by 10 K min^{-1} from RT to 723–823 K to desorb CO_2 from the catalyst surface into the He carrier stream while the CO_2 concentration was monitored with the mass spectrometer. The amount of CO_2 desorbed was quantified by comparing the area under the TPD curve to the peak areas of CO_2 calibration pulses injected after each experiment.

Reaction of 2-Propanol

The steady-state reaction of 2-propanol at atmospheric pressure was carried out in a single-pass, flow system operating at differential conversion (<5%). Liquid 2-propanol (Fisher, HPLC Grade) was pumped into a constant temperature vaporizer where it mixed with a flowing He stream (Roberts Oxygen, 99.99%) that was regulated by a mass flow controller. The He was used as received without additional purification; however, the alcohol reservoir was continuously sparged with He to remove dissolved gases. The 2-propanol/He mixture was fed to the reactor which was a quartz U-tube with a quartz frit to support the catalyst pellets and a thermocouple in contact with the catalyst, surrounded by a furnace. The vaporizer and all transfer lines were heated to about 400 K to prevent condensation in the system. Before loading the reactor, fresh catalyst was pressed without binder, crushed, and size separated to produce catalyst pellets with diameters between 0.25 and 0.42 mm. Typically 0.5–1.0 g of catalyst pellets were placed in the reactor, heated at a rate of 4 K min^{-1}, and calcined in a flowing helium stream before feeding 2-propanol. During our usual start-up procedure, the reactor was cooled to 593 K after calcination and a flowing 2-propanol/He mixture (1 : 1 molar ratio) bypassed the reactor until a steady flowrate was reached. Feed gases were then introduced to the catalyst bed and product gases were analyzed downstream by an on-line gas chromatograph with an FID detector. Since little change in 2-propanol conversion was observed after 1–2 h of operation, all rate data are reported after this steady state was achieved. The only products detected in significant quantity were propanone and propene. Therefore, product selectivities are defined by the number of moles produced of either propanone or propene divided by the total moles of propanone and propene. Activation energies and pre-exponential factors were determined from rate measurements over a temperature range of 573–613 K.

RESULTS

Catalyst Characterization

The elemental analyses for the Mg and Al contents of the synthetic hydrotalcites are shown in Table 1. As expected, the measured Mg : Al atomic ratios are very similar to the ratios in the original precipitation solutions. Results from X-ray diffraction confirmed that all of the hydrotalcites were successfully prepared without forming any separate phases. In addition, the *d*-spacing

TABLE 1

Bulk Elemental Analysis of as-Synthesized Hydrotalcites

Hydrotalcite sample[a]	Measured Mg : Al atomic ratio
HT5 : 1–K	4.57
HT3 : 1–K	3.09
HT2 : 1–K	1.87
HT5 : 1–Na	4.40
HT3 : 1–Na	3.00
HT2 : 1–Na	2.01

[a] Sample designation refers to the nominal Mg : Al atomic ratio expected from the synthesis conditions and to the method of preparation (K or Na precursors).

associated with the 003 peak in the hydrotalcite pattern, which is related to the interlayer spacing, decreased with increasing aluminum content and is consistent with earlier results for hydrotalcites with various Mg : Al ratios (*1*). The X-ray patterns of the precipitated aluminum hydroxide and calcined alumina showed both to be mixtures of different phases. To make proper comparisons, the synthesis conditions were similar to those used to form hydrotalcite. Therefore, optimization of the alumina synthesis procedure to obtain a pure phase was not performed.

The hydrotalcites were decomposed to give Mg(Al)O mixed oxides by heating in a helium stream to 723–923 K. Figure 1 shows a representative profile of CO_2 evolution from HT5 : 1–K during decomposition. Since the quantity of CO_2 represented by the area under the decomposition curve corresponded closely to half of the Al content in the sample, decomposition of the hydroxycarbonate is essentially complete above 650 K. However, residual surface hydroxyl groups may still be present. After calcination for 4 h, the resulting mixed oxides were examined by CO_2 temperature-programmed desorption in order to measure the density of surface base sites. The TPD profiles for MgO (Ube Industries), MgO from calcined $Mg(OH)_2$, HT5 : 1–K, HT3 : 1–K, and HT2 : 1–K, and Al_2O_3 are shown in Fig. 2 after calcination at 823 K. The profiles reveal a significant difference in CO_2 adsorption strengths between MgO and the calcined hydrotalcites. All the TPD curves have a peak at about 400 K, but both MgO samples also desorbed significant quantities of CO_2 at higher temperatures. Apparently, more high-strength base sites exist on the surfaces of the MgO catalysts than on the calcined hydrotalcites or alumina. The surface areas and base site densities for these materials are reported in Table 2. Magnesia has the lowest surface area (200 $m^2\ g^{-1}$) and alumina the greatest (290 $m^2\ g^{-1}$), while the surface areas of calcined hydrotalcites are in-between those of the pure materials. The base site densities measured by CO_2 TPD also varied with sample. The greatest density was found on Ube MgO (5.3×10^{-6} mol m^{-2}), followed by MgO exhydroxide (4.4×10^{-6} mol m^{-2}), then the calcined hydrotalcites (2-3 $\times$ 10^{-6} mol m^{-2}), and, as expected, the lowest base site density was measured on alumina (1.4×10^{-6} mol m^{-2}). No significant difference in surface areas or base site densities were measured for the calcined hydrotalcites prepared with Na precursors.

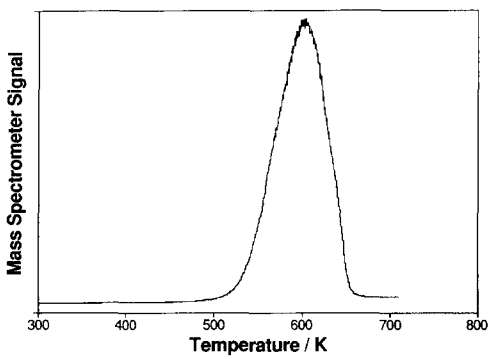

FIG. 1. Release of CO_2 from HT5 : 1–K during calcination in flowing He with a heating rate 4 K min^{-1}.

The magic-angle-spinning ^{27}Al NMR spectra of representative calcined hydrotalcites and alumina (calcined at 823 K) shown in Fig. 3 reveal that aluminum is coordinated to oxygen primarily in two environments.

The peak around 0 ppm is attributed to octahedrally coordinated aluminum, Al(o), and the peak around 50–80 ppm is attributed to tetrahedrally coordinated aluminum, Al(t) (*16*). The spectra in Fig. 3 compare the influence of preparation and Al content on the coordination geometry since (a) and (b) correspond to HT5 : 1–K and HT5 : 1–Na, respectively, and (c) and (d) correspond to HT2 : 1–K and HT2 : 1–Na, respectively. The spectrum for pure alumina is included in (e) for reference. Although accurate determination of a true Al(t)/Al(o) atomic ratio in a sample is complicated by asymmetric line broadening from secondary quadrupolar effects, general trends can be observed by simply comparing the integrated peak intensities. The Al(t)/Al(o) ratios estimated from the integrated peak intensities are 1.1 for HT5 : 1–K and 0.58 for HT5 : 1–Na. The Al(t)/Al(o) ratios are calculated to be 0.70 for HT2 : 1–K and 0.27 for HT2 : 1–Na. The Al(t)/Al(o) ratio for alumina is estimated to be 0.40. These results show that the proportion of Al(t) is influenced significantly by both the hydrotalcite preparation method and Al content. Both calcined hydrotalcite samples prepared with K have a greater proportion of Al(t) than their Na analogues, although the samples containing K and Na have nearly identical bulk compositions. In addition, a general trend of decreasing Al(t)/Al(o) with increasing Al content in the hydrotalcite samples prepared with the same

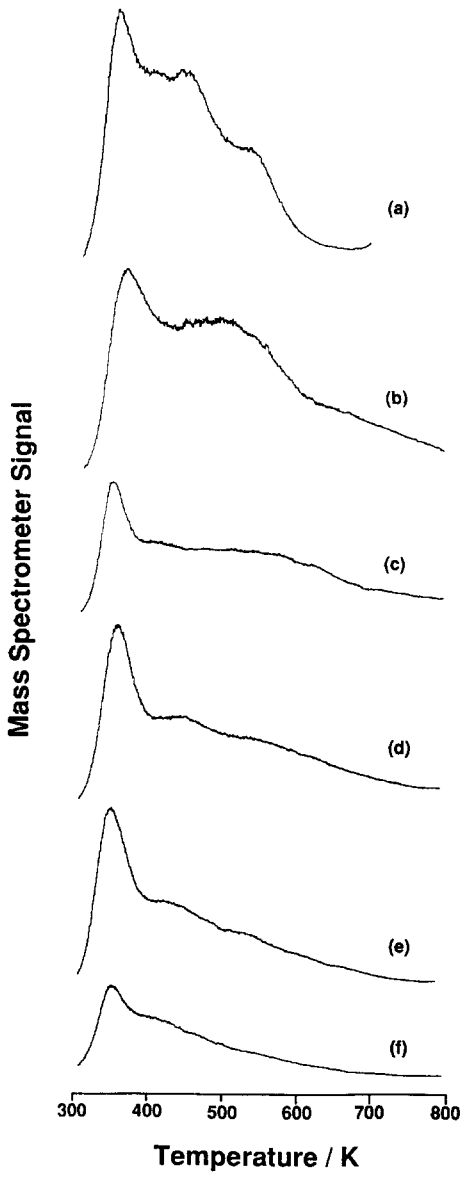

FIG. 2. CO_2 TPD profiles for (a) MgO, Ube Industries, (b) MgO ex-hydroxide, (c) HT5 : 1–K, (d) HT3 : 1–K, (e) HT2 : 1–K, and (f) Al_2O_3. A heating rate of 10 K min^{-1} was used and all samples were calcined at 823 K for 4 prior to TPD.

TABLE 2

Specific Surface Areas and Base Site Densities of Samples Calcined at 823 K

Sample	Surface area[a] (m^2 g^{-1})	Base site density[b] (10^{-6} mol m^{-2})
MgO[c]	200	4.4
MgO (Ube)[d]	100	5.3
HT5 : 1–K	230	2.2
HT3 : 1–K	210	2.9
HT2 : 1–K	230	2.8
HT5 : 1–Na	200	1.9
HT3 : 1–Na	220	2.2
HT2 : 1–Na	240	2.5
Al_2O_3	290	1.4

[a] Determined by N_2 adsorption.
[b] Determined by adsorption and TPD of CO_2.
[c] Magnesia prepared by calcination of $Mg(OH)_2$
[d] Magnesia from Ube Industries.

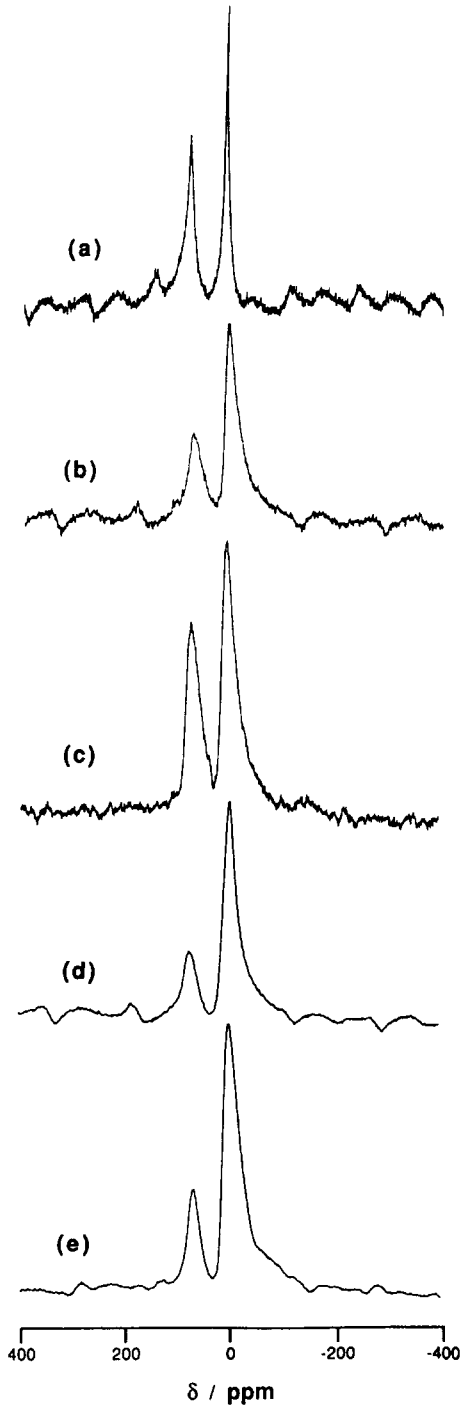

FIG. 3. ^{27}Al NMR spectra of representative aluminum containing samples after calcination at 823 K for 4 h. The spectra correspond to (a) HT5 : 1–K, (b) HT5 : 1–Na, (c) HT2 : 1–K, (d) HT2 : 1–Na, and (e) Al_2O_3.

precursors is also evident. Since the alumina sample was prepared with K, it also follows this trend.

The samples analyzed by magic-angle-spinning ^{27}Al NMR spectroscopy were then examined by X-ray photoelectron spectroscopy to determine the elemental composition of the surface region. The Mg : Al atomic ratios measured by XPS for calcined HT5 : 1–K and HT2 : 1–K were 2.4 and 1.5, respectively, although the overall bulk ratios for the same samples determined by elemental analysis were 4.57 and 1.87, respectively. Similar data were obtained for the Na samples. These results indicate that the surface regions of calcined hydrotalcites are enriched in Al. Additionally, the differences in the surface composition compared to the bulk composition are greater for the 5 : 1 samples than the 2 : 1 samples. The samples $Mg(OH)_2$, HT5 : 1–K, and HT5 : 1–Na were also analyzed for bulk K or Na and the maximum cation impurity levels {Imp/(Mg + Al + Imp)} were measured at 2 at.% for HT5 : 1–K. More importantly, the absolute surface concentrations of K and Na in HT5 : 1–K and HT5 : 1–Na were calculated from XPS to be 1.4 and 1.3 at.%, respectively, which demonstrates that the 5 : 1 hydrotalcites have nearly the same surface concentrations of impurity cations as well as Mg and Al.

Reaction of 2-Propanol

A linear variation of conversion with space time was observed over the range of conversions studied (0–5%) confirming that the reactor operated in a differential mode. In addition, heat and mass transfer correlations verified that no significant inter- and intraparticle gradients exist at the conditions used. Varying the alcohol partial pressure betwen 30 and 70 kPa did not affect the observed rate over calcined hydrotalcite. Therefore, the decomposition of 2-propanol can be considered a zero-order reaction over these materials.

Kinetic results from the reaction of 2-propanol over hydrotalcites calcined for 4 h at

TABLE 3

Steady-State Reaction Rates for the Conversion of 2-Propanol at 593 K

Catalyst	Calcination temperature[a] (K)	Rate of propanone formation (10^{-9} mol m^{-2} s^{-1})	Selectivity to propanone[b] (%)
MgO	723	16	97
HT5 : 1–K	723	11	90
HT3 : 1–K	723	6.5	85
HT2 : 1–K	723	6.1	74
MgO(Ube)	823	31	84
MgO	823	12	97
HT5 : 1–K	823	7.3	94
HT3 : 1–K	823	6.7	84
HT2 : 1–K	823	7.5	70
HT5 : 1–Na	823	11	58
HT3 : 1–Na	823	8.7	66
HT2 : 1–Na	823	7.4	51
Al_2O_3	823	2.7	2.5
MgO/Al_2O_3(3 : 1)[c]	823	8.2	17
MgO	923	13	96
HT5 : 1–K	923	3.3	88
HT3 : 1–K	923	5.1	76
HT2 : 1–K	923	5.9	64
HT3 : 1–K	1173	1.7	54

[a] Calcination was carried out in flowing He for 4 h at the indicated temperarture.

[b] Selectivity is defined as the rate of formation of propanone divided by the sum of rates of formation of propanone and propene.

[c] This sample is made by physically mixing pure MgO and Al_2O_3 in a 3 : 1 Mg : Al atomic ratio.

various temperatures are presented in Table 3. Reaction rates and selectivities are reported at a common temperature of 593 K for typical conversions of 1–3%. The specific rate of propanone formation was greatest over the Ube MgO catalyst (31 × 10^{-9} mol m^{-2} s^{-1}) exceeding by about a factor of 2 the rate over MgO prepared by calcination of $Mg(OH)_2$ (12-16 × 10^{-9} mol m^{-2} s^{-1}). The propanone formation rates over the hydrotalcites calcined at 723-923 K ranged from 3.3 to 11 × 10^{-9} mol m^{-2} s^{-1} which are similar to the rates measured over MgO ex-hydroxide. The selectivity to propanone formation was greatest over MgO ex-hydroxide (97%).

The selectivity to propanone over calcined hydrotalcites was influenced by both the aluminum content and preparation method. For the hydrotalcites prepared with K precursors, the propanone selectivity decreased as Al content increased. However, no trend in propanone selectivity with aluminum content was observed over calcined hydrotalcites prepared with Na. Also, the selectivities over hydrotalcites prepared with Na were generally poorer than those measured for the K samples at identical conditions. Even though Na and K were detected in small amounts by XPS, we believe that 2-propanol reacts primarily on Mg(Al)O surface sites and not on the highly basic oxides of Na and K. The nearly constant rates of propanone formation over MgO and calcined hydrotalcites (Table 3) support this conclusion.

The specific rate of propanone formation over HT3 : 1-K calcined at 1173 K was 1.7 × 10^{-9} mol m^{-2} s^{-1} and the propanone selectivity was 54%, both of which are significantly less than the values measured for HT3 : 1–K calcined in the temperature range of 723–923 K. In addition, high-temperature calcination reduced the surface area (compared to low-T calcination) and caused the formation of crystalline spinel which was detected by X-ray diffraction.

The activation energy, E_a, and pre-exponential factor, A, for propanone and propene formation were calculated from rate measurements over the temperature range 573–613 K. As shown by the representative data in Figs. 4 and 5, the Arrhenius plots are markedly linear over the range of tempera-

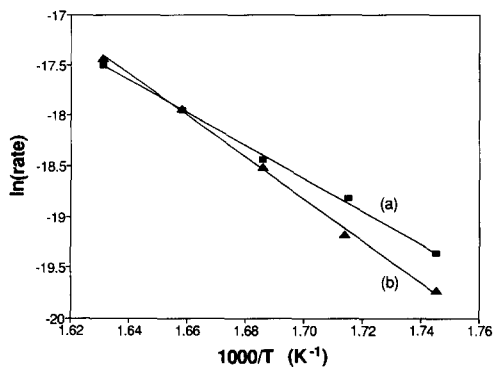

FIG. 4. Variation of the propanone formation rate (mol m^2 s^{-1}) with temperature over (a) MgO, ex-hydroxide, and (b) HT5 : 1–K, both calcined at 823 K.

tures studied which is consistent with a lack of transport effects on the kinetic data. Values of the activation energies and pre-exponential factors for reactions over MgO, calcined hydrotalcites, and alumina (all calcined at 823 K) are reported in Table 4.

Several interesting observations are noted. First, the lowest activation energies and pre-exponential factors for propanone formation were calculated for pure MgO and Al_2O_3. However, for the hydrotalcite series prepared with K, both A and E_a significantly increased from the values measured for the pure oxides. For example, the pre-exponential factor and activation energy for HT5 : 1–K were greater than the respective values for MgO by about four orders of magnitude and 40 kJ mol^{-1}. In addition, both A and E_a decreased as the aluminum content of the hydrotalcites increased. These trends for the K series hydrotalcites were also observed for samples calcined at 723 and 923 K, demonstrating that the results are reproducible. For the materials prepared with Na, no influence of Al content on E_a and A was observed, but the Arrhenius parameters were greater than those calculated for pure MgO.

The lowest activation energy for propene formation was calculated for pure alumina. The activation energies and pre-exponential factors for the calcined hydrotalcites were greater over the K-prepared samples than those prepared with Na. In fact, the activation energies found over the K series were similar to the value calculated for pure MgO. The E_a and A for propene formation over both the K and Na series calcined hydrotalcites were little affected by the aluminum content of the sample.

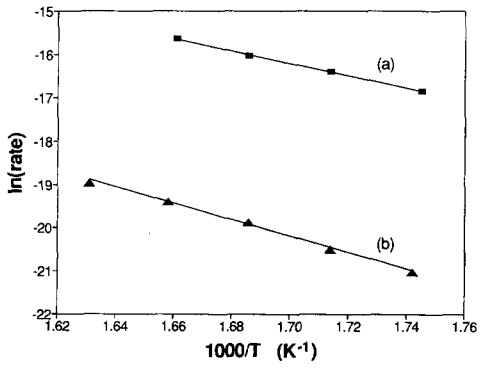

FIG. 5. Variation of the propene formation rate (mol m^2 s^{-1}) with temperature over (a) Al_2O_3 and (b) HT2 : 1–K, both calcined at 823 K.

DISCUSSION

The coprecipitation conditions used in this work satisfactorily produced magnesium aluminum hydroxycarbonates with the desired compositions. Reichle reports that coprecipitation of Mg and Al salts results in hydrotalcite crystals for Mg : Al atomic ratios of about 2–4 (*17*). For compositions outside that range, hydroxides of Al and Mg can form in the product. We found no evidence of crystalline phases other than hydrotalcite over the entire range of Mg : Al atomic ratios from 1.9 to 4.6. In addition, recent work by Shaper *et al.* demonstrates that nearly pure hydrotalcite can be synthesized with Mg : Al of 10 : 1 if the coprecipitation is performed under strictly controlled conditions of mixing, temperature, and pH (*1*).

The thermal decomposition of hydrotalcites has been studied previously in great detail (*4, 5*). In general, hydrotalcite loses interlayer water after heating to about 400–600 K. Above about 600 K, increases in specific surface area and pore volume result from evolution of structural water and CO_2. The X-ray diffraction patterns of materials calcined between 600 and 800 K may show both MgO and HT crystal structures, indicating that decomposition is incomplete. However, only the magnesia crystal structure is detected in materials calcined at temperatures near 800 K. These mixed oxides are metastable since very-high-temperature calcination (~1200 K) causes the formation of the separate oxide phase $MgAl_2O_4$ as well as MgO (*5*).

Hydrotalcites were usually calcined at temperatures between 723 and 923 K which is in the range where hydroxycarbonate

TABLE 4

Pre-exponential Factors and Activation Energies for the Formation of Propanone and Propene from 2-Propanol[a]

Catalyst	A Propanone (10^4 mol m^{-2} s^{-1})	E_a Propanone (kJ mol^{-1})	A Propene (10^4 mol m^{-2} s^{-1})	E_a Propene (kJ mol^{-1})
MgO	0.73	134	(4)[b]	(160)[b]
HT5 : 1–K	940	172	(97)[b]	(174)[b]
HT3 : 1–K	67	159	25	163
HT2 : 1–K	6.2	146	68	160
HT5 : 1–Na	8.3	146	1.0	126
HT3 : 1–Na	12	149	0.71	137
HT2 : 1–Na	12	150	0.52	133
Al_2O_3	(0.41)[b]	(138)[b]	2.6	118

[a] All samples were calcined at 823 K for 4 h in flowing He.

[b] Values in parentheses are not considered as reliable as the other values in the table since very small amounts of the product were formed at low temperatures.

completely decomposes without forming crystalline spinel. Gas-phase CO_2 was monitored during decomposition in order to determine the temperature at which decarbonation was complete. As shown in Fig. 1, HT5 : 1–K released all the interlayer carbonate by 650 K, which is consistent with the description of thermal decomposition given above. In addition, X-ray diffraction patterns of the calcined materials showed that the MgO structure was generated, confirming that decomposition was complete. These activated materials were then investigated by CO_2 TPD, ^{27}Al NMR, XPS, and reaction of 2-propanol.

The fraction of total surface lattice oxide atoms that are surface base sites can be estimated from the results in Table 2. If the surface of MgO powder is assumed to preferentially expose the (100) face and if the Mg-O interatomic distance is the crystal bond distance of 0.21 nm, then the surface lattice oxide density is 1.1×10^{15} atoms cm^{-2}. Therefore, about one-quarter of the surface lattice oxygen atoms of the MgO ex-hydroxide and MgO from Ube Industries act as surface base sites for the adsorption of CO_2. This compares to 10% found by Kurokawa *et al.*, who studied CO_2 TPD from MgO that was pretreated at 873 K for 2 h in He (*18*). In addition, Choudhary and Pandit investigated the influence of $Mg(OH)_2$ preparation and calcination on the capacity for CO_2 adsorption (*19*). For an hydroxide sample prepared and calcined at conditions similar to those described in Table 2, they report a total base site density of 4.6×10^{-6} mol m^{-2}, which corresponds to about one quarter of the total surface lattice oxide density and is in excellent agreement with the basicity of MgO ex-hydroxide reported in this work. The base site densities of the calcined hydrotalcites are about half of the value measured for pure MgO and correspond to about 10–15% of the total surface oxide atoms, assuming that the oxide density is about the same as that of pure MgO. Since the X-ray diffraction patterns of all calcined hydrotalcites revealed a slightly distorted MgO structure, the surface oxide concentration is probably similar to that of pure MgO.

The results from CO_2 TPD also indicate the relative strengths of the surface base sites. The TPD curves from both MgO samples in Fig. 2 show a desorption peak at relatively low temperature and a significant broad shoulder at higher temperatures. In fact, the CO_2 associated with the high temperature shoulder is at least half the total amount of adsorbed CO_2 on MgO. How-

ever, the number of high-temperature adsorption sites is lower on the Mg(Al)O samples than on the pure MgO samples. This loss of high-temperature, or high-strength, surface base sites is largely responsible for the decrease in basicity measured for the calcined hydrotalcites (Table 2). Apparently, the incorporation of Al into the precursor materials alters the final basicity by inhibiting the formation of strongly basic surface sites. Kurokawa *et al.* report that the total base site density of MgO impregnated with Al is an order of magnitude lower than that of pure MgO (*18*), which is far lower than any differences between the calcined hydrotalcites and MgO reported here. In fact, Table 2 shows that pure alumina has a CO_2 adsorption capacity one third the value of pure magnesia.

Magic-angle-spinning ^{27}Al NMR spectroscopy was used to investigate the chemical environment of Al in the Mg(Al)O structure. The spectra of Fig. 3 show that both octahedrally and tetrahedrally coordinated Al exist in all the mixed oxides as well as pure alumina. The pure alumina spectrum is similar to those obtained by Slade *et al.* (*16*) and John *et al.* (*20*), who studied the thermal transformations of alumina hydrates by ^{27}Al NMR spectroscopy. Dehydration of both bayerite and boehmite at 800–900 K (the conditions used in this work) results in aluminas with Al(t)/Al(o) ratios of 0.3–0.4, which are close to the value of 0.40 measured in this work (*20*). John *et al.* speculate that the large amount of tetrahedral species observed in transitional aluminas may result from the typically high specific surface areas of calcined hydrates which expose a significant fraction of Al to the surface (*20*). Additionally, the defect spinel structure of γ-alumina accounts for the presence of both tetrahedral and octahedral Al in a ratio of 0.33 (*16*).

The situation is very different for the mixed oxides. A significant fraction of tetrahedrally coordinated Al is also present in the mixed oxides and in most cases exceeds that of pure alumina. Since only peaks associated with MgO were detected in the X-ray diffraction patterns of the calcined hydrotalcites, no separate, crystalline, spinel phases exist that could account for the tetrahedral aluminum. However, an amorphous phase not detected by X-ray diffraction may contribute to the observed Al(t) peak. If the Al was distributed randomly throughout the Mg(Al)O crystals, it is expected that the Al(t)/Al(o) ratio would be less than that of pure alumina since the surface areas of the calcined hydrotalcites were less than that of alumina, thus exposing fewer Al atoms to the surface. However, our XPS results show that the Mg : Al ratio at the surface is less than the bulk composition, indicating that the Al is not randomly distributed but instead concentrates near the surface. Therefore, the tetrahedral peak may be produced by surface Al. Reichle also observed the presence of Al(t) by NMR and measured an increase in Al surface concentration by XPS for hydrotalcite calcined at 723 K (*4*). In addition, Reichle reports that the surface Mg : Al ratio is a fairly strong function of calcination temperature but does not speculate on the mechanism for the reorganization of the surface (*4*). Derouane *et al.* propose that high Al(t)/Al(o) ratios in calcined hydrotalcites result from Al migration to interstitial sites of tetrahedral symmetry (*21*). Our comparison of the K-samples with the Na-samples in Fig. 3 shows that the method of hydrotalcite preparation also affects the extent at which Al is tetrahedrally coordinated. Why this is the case is not yet clear.

The reaction of 2-propanol was used to probe the surface reactivity of calcined hydrotalcites. Generally, 2-propanol dehydrogenates to propanone over basic catalysts and dehydrates to propene over acidic catalysts (*13, 14*). Therefore, the selectivity of the 2-propanol reaction measures the relative acidity and basicity of the mixed oxides compared to the pure materials. As expected, the selectivity favored propanone (97%) over basic MgO and propene (98%) over acidic Al_2O_3. However, the rate and selectivity of the reaction over calcined hy-

drotalcites depended on many factors, including Mg : Al atomic ratio, method of preparation, and calcination temperature.

The rates of propanone formation catalyzed by hydrotalcites calcined at 723–923 K were essentially the same, varying by less than a factor of two. Also, the rates over the mixed oxides equalled approximately half the rate over pure MgO. The specific rates of propanone formation over magnesium hydroxide and MgO (Ube) calcined at 823 K were 12×10^{-9} and 31×10^{-9} mol m^{-2} s^{-1}, respectively. These values compare to 2.1×10^{-9} mol m^{-2} s^{-1} (*22*), 2.0×10^{-9} mol m^{-2} s^{-1} (*23*), and 25×10^{-9} mol m^{-2} s^{-1} (*24*) measured over MgO and converted to our conditions. If sufficient data were not provided in the cited papers, then the rates were calculated from the activation energy measured in this work assuming a zero order reaction. Our specific rates over calcined hydrotalcites fall within the range of values reported for pure MgO. In addition, the selectivity toward propanone over all hydrotalcite samples was greater than 50%, indicating that little acidity at the surface is produced by aluminum incorporation. To confirm this result, 2-propanol was reacted over a physical mixture of MgO/Al_2O_3 (Mg : Al = 3) and the selectivity was compared to that obtained over a calcined hydrotalcite with the same Mg : Al ratio. The selectivities for propanone formation over MgO/Al_2O_3 and HT3 : 1–K (see Table 3) are 17 and 84%, respectively, confirming the lack of significant acidity on the hydrotalcite surface. Apparently, Al^{3+} located primarily in a MgO lattice is less active for dehydration relative to alumina.

Since results from ^{27}Al NMR spectroscopy and XPS indicate that Al concentrates at the surface of calcined hydrotalcites, we conclude that the surface Al is in a local oxidic environment that does not favor acid-catalyzed reactions that typically occur over pure alumina.

The influence of hydrotalcite preparation on selectivity can partially account for the observation of Kelkar *et al.* that both dehydrogenation and dehydration of 2-propanol occur over calcined hydrotalcite (Mg/Al = 3) at comparable reaction temperatures (*8*). Most of the samples in their study were prepared by coprecipitation of nitrate salts with NaOH; however, the selectivities for propanone formation shown in Table 3 over catalysts prepared using NaOH were significantly less than those of samples prepared using KOH, but were similar to the values reported by Kelkar *et al.* (*8*). In addition, Kelkar et al. observed very little tetrahedrally coordinated Al by NMR in their hydrotalcite after calcination at 723 K unlike the rather large fraction of Al(t) reported in this work. Apparently, direct comparison of calcined MgAl oxides is complicated by the sensitivity of surface properties to preparation conditions.

TABLE 5

The Compensation Effect for Propanone Formation over Calcined Hydrotalcites

Catalyst	A Propanone[a] (s^{-1})	E_a Propanone (kJ mol^{-1})
HT5 : 1–K	4.3×10^{12}	172
HT3 : 1–K	2.3×10^{11}	159
HT2 : 1–K	2.2×10^{10}	146
MgO	1.6×10^{9}	134

[a] Pre-exponential factors were calculated from the values reported in Table 4 (823 K) normalized by the base site densities in Table 2.

The origin of the compensation effect for propanone formation over the hydrotalcite series prepared with K precursors is not entirely clear. Since the activation parameters were determined near the isokinetic temperature, it could be argued that variations in A and E_a are due to scatter in the data (*25*); however, the reported values are reproducible and the Arrhenius plots shown in Figs. 4 and 5 are linear. If the active site density is assumed to approximately equal the base site density measured by CO_2 TPD, then the pre-exponential factors equal the values in Table 5. This assumption is partially justified by the results of Peng and Barteau, who

probed the reactivity of surface acid–base pairs on magnesia (*26*). They reported a coverage of 0.34 for methanol dissociatively adsorbed on a sputtered MgO (100) surface at 300 K. This compares to our estimate that one-quarter of the MgO powder surface is covered by CO_2. The largest pre-exponential factor of 4.3×10^{12} s^{-1} for HT5 : 1–K is near the value of $kT/h \sim 10^{13}$ s^{-1} expected from transition state theory for a unimolecular, surface reaction (*27*). However, the value of the pre-exponential factor decreases by three orders of magnitude over the series in Table 5, with that of MgO being the lowest. Since surface areas and base site densities vary by only a factor of 2 throughout the series, we believe that the decrease in pre-exponential factor cannot be accounted for by a three orders of magnitude decrease in active site concentration.

A possible explanation for a variation in A and E_a is a shift in the rate-determining step. The sequence of elementary steps for the dehydrogenation of 2-propanol over basic oxides is generally believed to begin with the dissociative chemisorption of alcohol to give surface alkoxide (isopropoxide) and a hydrogen atom (*28*, *29*). The later steps probably include: (2) removal of the second hydrogen from adsorbed isopropoxide giving adsorbed propanone; (3) hydrogen atom recombination and desorption; and (4) propanone desorption. Szabó *et al.* also observed a compensation effect for the reaction of 2-propanol over MgO, CaO and SrO, where the pre-exponential factor over MgO was three orders of magnitude less than that over SrO and four orders of magnitude less than that over CaO (*22*). They explained the variation of A by a shift in rate-determining step from alkoxide dehydrogenation over MgO to propanone desorption over CaO and SrO and we can apply their reasoning to the results in Table 5. The pre-exponential factor for the observed zero-order reaction can be written from transition state theory as $[(kT/h) \cdot \exp(\Delta S^{\circ\dagger}/R)]$, where $\Delta S^{\circ\dagger}$ is the molar entropy of formation of the transition state at the standard state and R is the gas constant. The quantity $\Delta S^{\circ\dagger}/R$ for the removal of hydrogen from adsorbed isopropoxide is likely to be negative since the transition state probably has fewer rotational and vibrational modes than the adsorbed alkoxide. In fact, Szabo *et al.* estimate the pre-exponential factor for this step to be 10^8 s^{-1}, which is close to the value reported in Table 5 for propanone formation over MgO (*22*). Since the pre-exponential factor for HT5 : 1–K is obtained by assuming $(\Delta S^{\circ\dagger}/R) \sim 0$, the rate-determining step over this catalyst may be the unimolecular desorption of propanone. Also, propanone adsorbed on basic oxides such as MgO and ZnO is known to form a stable surface enolate species (*28–31*). Although incorporation of aluminum into MgO suppresses the formation of strong basic sites as measured by CO_2 TPD, the presence of Al^{3+} at the surface of Mg(Al)O may stabilize the formation of strongly bound propanone thereby altering the overall steady-state kinetics of alcohol decomposition.

Temperature-programmed desorption of propanone from the Zn(0001) polar surface of ZnO indicates that propanone can be strongly adsorbed on a metal oxide (*31*). After preadsorption of propanone at 300 K, the TPD spectrum exhibited a peak maximum at ~450K, with a significant tail at higher temperatures. The activation energy for propanone desorption is calculated to be 120 kJ mol^{-1} using the equation of Redhead and assuming a pre-exponential factor of 10^{13} s^{-1} (*32*). In addition, the propanone desorption peak maximum in the temperature-programmed reaction profile of 2-propanol adsorbed on Zn(0001) is 455 K, suggesting that the rate constant for dehydrogenation of adsorbed alkoxide is similar to that of propanone desorption. These results are consistent with the observation in this work of nearly equivalent rates of 2-propanol dehydrogenation over MgO and calcined hydrotalcites even though the rate-determining step may shift throughout the catalyst series.

The concept of a nonuniform surface on

the catalyst powders may further explain how pre-exponential factors can be between the two extremes found for MgO and HT5 : 1–K. Zwicker *et al.* (*33*) and Vohs and Barteau (*31*) studied the decomposition of 2-propanol over the polar faces of ZnO single crystals and found that reactivity was highly dependent on the exposed crystal plane. Results from work with single crystals indicate that metal cations at the surface are necessary to form the active site since the oxygen-terminated surface is completely inactive for reaction. In contrast, Djéga-Mariadassou *et al.* reported that 2-propanol decomposition over oriented ZnO powders is structure insensitive (*34*). The propanone formation rates in Table 3 may initially suggest that the reaction over MgO and calcined hydrotalcites is also structure-insensitive. However, as discussed above, these results are measured near the isokinetic temperature so that rates over all samples are nearly equivalent. Also, since catalyst powders have many different crystal planes that expose cations and anions in various states of coordination, we do not believe that structure sensitivity or insensitivity of alcohol decomposition over oxide materials can be easily inferred by comparing rates over different catalyst powders. However, our results showing different CO_2 adsorption sites on the various MgO and Mg(Al)O materials indicate that the surfaces of the catalysts are nonuniform. Also, single-crystal studies demonstrate conclusively that the 2-propanol decomposition is extremely sensitive to surface structure and justify the evaluation of the overall reaction kinetics in the framework of a nonuniform surface.

The two-step sequence of surface reactions for the formation of propanone from 2-propanol over MgO and Mg(Al)O is proposed

$$(\text{alkoxide})_{ads} \rightarrow \ldots\ldots \qquad (1)$$

$$\ldots\ldots$$

$$(\text{propanone})_{ads} \rightarrow \ldots\ldots, \qquad (2)$$

where (1) corresponds to the removal of the second hydrogen atom from the adsorbed alkoxide with rate constant k_1 and (2) corresponds to the desorption of propanone with rate constant k_2. All other steps and surface intermediates are considered to be kinetically insignificant. From the kinetic treatment of two step reactions over nonuniform surfaces developed by Temkin (*35*), we can write for a total surface site density $[L]$:

$$v = \tau [L] \frac{k_1^0 k_2^0}{(k_1^0)^m (k_2^0)^{1-m}}, \qquad (3)$$

where the superscript zero refers to the values of the rate constants on sites having the greatest affinity for the reaction and τ is an integration constant of order 1. The exponent m is the difference of two terms with physical meanings, $m = \alpha - \gamma$, where α is a transfer coefficient or Brønsted parameter that can vary from 0 to 1 and γ is related to the distribution of sites on the surface. A linear distribution of sites corresponds to $\gamma = 0$. The reaction rate is independent of the gas-phase 2-propanol concentration which agrees with the experimental results. For $m = 1$, the rate expression in (3) reduces to the rate of step (2), the desorption of propanone, and the preexponential factor is expected to be 10^{13} s^{-1}. At the other extreme, for m = 0, the overall rate is equal to the rate of step (1), the dehydrogenation of adsorbed alkoxide, and the pre-exponential factor is expected to be lower than 10^{13} s^{-1} as discussed earlier. These two limits may explain the observed pre-exponential factors over HT5 : 1–K and MgO and are consistent with the recent definition proposed by Boudart and Tamaru for a rate determining step of a catalytic sequence with two exergic steps (*36*). In addition, modification of the surface nonuniformity by additional aluminum incorporation can result in different values for m ($0 < m < 1$) which would give preexponential factors between the values for steps (1) and (2) without assuming the existence of a single rate-determining step.

The compensation effect for propanone formation was not observed over the hydro-

talcites prepared with Na. The K series and Na-series differed in several important respects. First, ^{27}Al NMR spectroscopy revealed that a lower fraction of the total Al in the Na samples was tetrahedrally coordinated. Second, the selectivity to propanone formation was lower over the Na series. And finally, the activation energies for propene formation over the Na catalysts are at least 30 kJ mol^{-1} lower than the corresponding K catalysts as compared to an estimated 40 kJ mol^{-1} difference in propene activation energies over MgO and Al_2O_3 (Table 4) with alumina having the lower value. These differences can be explained by an inhomogeneous distribution of Al at the surface of the Na-series hydrotalcites. If some surface regions were rich in Al and other regions rich in Mg, then the overall catalytic reaction of 2-propanol would appear as the superposition of reactions occurring over each region. This interpretation is supported by experiments with HT3 : 1–K calcined at 1173 K. The selectivity to propanone for HT3 : 1–K calcined at 1173 K was only 54% but was about 85% for hydrotalcite calcined at lower temperatures (Table 3). Since X-ray diffraction indicated that a separate Al-rich spinel phase formed after high-T calcination, we attribute the production of propene to that phase. Apparently, preparation of hydrotalcites with K precursors yields a calcined mixed oxide in which Al is more evenly distributed at the surface. Also, the direct participation of the impurity cations (K) in the reaction sequence cannot be entirely ruled out and may actually contribute to the nonuniformity of the surface.

CONCLUSIONS

Magnesium–aluminum mixed oxides derived from hydrotalcite precursors exhibit surface basicities as measured by CO_2 TPD and 2-propanol decomposition similar to pure magnesia. Although aluminum in the as-synthesized hydrotalcite is probably well distributed throughout the lattice, calcination produces a concentration of Al at the surface that is greater than the overall bulk composition; however, this surface Al^{3+} is in a tetrahedrally coordinated oxidic environment that does not significantly catalyze the formation of propene from 2-propanol unlike pure alumina. Large differences in the ^{27}Al NMR spectra and catalytic activity of calcined hydrotalcites prepared under different conditions demonstrate the influence of the synthesis method on the final properties of the calcined materials. Results from the decomposition of 2-propanol indicate that Al is distributed more homogeneously on the surface of the mixed oxides prepared with K precursors than on samples prepared with Na precursors. Since aluminum incorporation into MgO reduces the number of high-strength CO_2 adsorption sites, we speculate that the distribution of surface catalytic sites is also affected. Therefore, the observed compensation effect for propanone formation over hydrotalcites prepared with K can be explained by a two-step surface reaction sequence occurring on a nonuniform surface.

ACKNOWLEDGMENTS

This work was supported by the National Science Foundation (Grant CTS-9108206). We also thank Professor John Dillard for providing XPS analysis of the hydrotalcite samples, and Chris French for help in synthesizing some of the materials used in this work. Professor David Cox is acknowledged for his critical review of this manuscript and helpful suggestions.

REFERENCES

1. Schaper, H., Berg-Slot, J. J., and Stork, W. H. J., *Appl. Catal.* **54,** 79 (1989).
2. Miyata, S., and Kumura, T., *Chem. Lett.,* 843 (1973).
3. Drezdzon, M. A., *in* "Symposium on New Catalytic Materials and Techniques, Am. Chem. Soc. Miami Beach Meeting, Sept 10–15, 1989," p. 511.
4. Reichle, W. T., Kang, S. Y., and Everhardt, D. S., *J. Catal.* **101,** 352 (1986).
5. Miyata, S., *Clays Clay Miner.* **28,** 50 (1980).
6. Reichle, W. T., *J. Catal.* **94,** 547 (1985).
7. Nakatsuka, T., Kawasaki, H., Yamashita, S., and Kohjiya, S., *Bull. Chem. Soc. Jpn.* **52,** 2449 (1979).
8. Kelkar, C. P., Schutz, A., and Marcelin, G., *in* "Perspectives in Molecular Sieve Science" (W. H. Flank and T. E. Whyte, Eds.), p. 324. Am. Chem. Soc., Washington, DC, 1988.
9. Corma, A., Fornés, V., Martin-Aranda, R. M., and Rey, F., *J. Catal.* **134,** 58 (1992).

10. Davis, R. J., and Derouane, E. G., *Nature* **349,** 313 (1991).
11. Davis, R. J., and Derouane, E. G., *J. Catal.* **132,** 269 (1991).
12. Cavani, F., Trifirò, F., and Vaccari, A., *Catal. Today* **11,** 173 (1991).
13. Gervasini, A., and Auroux, A., *J. Catal.* **131,** 190 (1991).
14. Krylov, O. V., "Catalysis by Nonmetals," p. 115. Academic Press, New York, 1970.
15. Marsuura, I., Hashimoto, Y., Takayasu, O., Nitta, K., and Yoshida, Y., *Appl. Catal.* **74,** 273 (1991).
16. Slade, R. C. T., Southern, J. C., and Thompson, I. M., *J. Mater. Chem.* **1,** 875 (1991).
17. Reichle, W. T., *Solid State Ionics* **22,** 135 (1986).
18. Kurakawa, H., Kato, T., Kuwabara, T., Ueda, W., Morikawa, Y., Moro-oka, Y., and Ikawa, T., *J. Catal.* **126,** 208 (1990).
19. Choudhary, V. R., and Pandit, M. Y., *Appl. Catal.* **71,** 265 (1991).
20. John, C. S., Alma, N. C. M., and Hays, G. R., *Appl. Catal.* **6,** 341 (1983).
21. Derouane, E. G., Julien-Lardot, V., Davis, R. J., Blom, N., and Højlund-Nielsen, P. E., submitted.
22. Szabó, Z. G., Jóvér, B., and Ohmacht, R., *J. Catal.* **39,** 225 (1975).
23. McCaffrey, E. F., Micka, T. A., and Ross, R. A., *J. Phys. Chem.* **76,** 3372 (1972).
24. Hathaway, P. E., and Davis, M. E., *J. Catal.* **116,** 263 (1989).
25. Boudart, M., "Kinetics of Chemical Processes," p. 179 Prentice-Hall, Englewood Cliffs, NJ, 1968.
26. Peng, X. D., and Barteau, M. A., *Langmuir* **7,** 1426 (1991).
27. Boudart, M., and Djéga-Mariadassou, G., "Kinetics of Heterogeneous Catalytic Reactions," p. 62. Princeton Univ. Press, Princeton, NJ, 1984.
28. Koga, O., Onishi, T., and Tamaru, K., *J. Chem. Soc. Faraday Trans. 1* **76,** 19 (1980).
29. Akiba, E., Soma, M., Onishi, T., and Tamaru, K., *Z. Phys. Chem. Neue Folge* **119,** 103 (1980).
30. Miyata, H., Toda, Y., and Kubokawa, Y., *J. Catal.* **32,** 155 (1974).
31. Vohs, J. M., and Barteau, M. A., *J. Phys. Chem.* **95,** 297 (1991).
32. Redhead, P. A., *Vacuum* **12,** 203 (1962).
33. Zwicker, G., Jacobi, K., and Cunningham, J., *Int. J. Mass Spectrom. Ion Processes* **60,** 213 (1984).
34. Djéga-Mariadassou, G., Davignon, L., and Marques, A. R., *J. Chem. Soc. Faraday Trans. 1* **78,** 22447 (1982).
35. Boudart, M., and Djéga-Mariadassou, G., "Kinetics of Heterogeneous Catalytic Reactions," p. 118. Princeton Univ. Press, Princeton, NJ, 1984.
36. Boudart, M., and Tamaru, K., *Catal. Lett.* **9,** 15 (1991).